Vol 16 No 11, November 2007
1009-1963/2007/16(11)/3464-06
Chinese Physics
© 2007 Chin. Phys. Soc.
and IOP Publishing Ltd

Effects of trapped electrons on off-axis lower hybrid current drive in tokamaks*

Jiao Yi-Ming(焦一鸣)†, Long Yong-Xing(龙永兴), Dong Jia-Qi(董家齐),
Gao Qing-Di(高庆弟), Wang Ai-Ke(王爱科), and Liu Yong(刘 永)

Southwestern Institute of Physics, Chengdu 610041, *China*

(Received 21 July 2006; revised manuscript received 26 February 2007)

The effects of trapped electrons on off-axis lower hybrid current drive (LHCD) in tokamaks are studied, A computer code for solving the Fokker–Planck equation in a toroidal geometry is developed and employed. The code is suitable for various auxiliary heating and current drive schemes in tokamak plasmas. The influence of the resonance regime on the current drive efficiency as well as the influence of trapped particle fraction on the current drive efficiency are emphasized. It is shown that, as an electrostatic force, the lower hybrid wave causes some of the trapped electrons to be untrapped and lose their energy, which can cut the LHCD efficiency by about 30%. The ITER scaling law is also used to estimate the trapped electron effects.

Keywords: trapping electron effect, off-axis lower hybrid current drive
PACC: 5250 5255, 5265

1. Introduction

As good auxiliary methods, lower hybrid wave heating (LHH) and lower hybrid current drive (LHCD) have been successfully investigated in tokamak experiments, such as JET, TORE-SUPRA, and TRIAM-1M.[1−3] With the application basis established in the early 80's of the last century through theoretical and experimental studies, an MW and MA level of LHCD is achievable in experiments[4,5] nowadays. This is close to the LHCD requirement for higher current drive efficiency and higher plasma density in fusion reactors.

In the review papers of Fish,[6,7] the basic theories of LHH and LHCD are presented. The theories and experiments have demonstrated that lower hybrid (LH) waves interact efficiently with electrons in the high energy tail of their distribution in velocity space. Brambilla's spectrum determines the injected wave resonance regime and its power distribution.[8] One can obtain the resonance regime $[n_{//\,\mathrm{min}}, n_{//\mathrm{Max}}]$ from the spectrum and use it as the initial values in a ray tracing code.[9,10] The regime corresponds to $[v_{//1}, v_{//2}]$ in the velocity space, where $v_{//} = c/n_{//}$. For a tokamak equilibrium with poloidal inhomogeneity and axial symmetry, the poloidal mode number of the waves is not conserved,[11] whereas the toroidal mode number is a constant of the wave motion, i.e. along a ray trajectory wave momentum changes, and there exist various $k_{//}$ resonance regimes at different magnetic surfaces. This enables us to choose a suitable resonance regime at a magnetic surface for optimizing driven current profile.

Trapped electron effect is an issue for LHCD. Since particle trapping effects become more important at larger plasma radii, they negatively impact the power requirements for off-axis current drive using LHCD. Toroidal drifts of the trapped electrons have a block effect on lower hybrid current drive. This part of electrons has lower toroidal velocities after magnetic surface has been averaged, and absorbs more injected LH wave energy. This is not in favour of lower hybrid current drive. Yoshioka and Antonsen[12] derived a bounce averaged 2D Fokker–Planck equation, and analysed the neoclassical effects on the current drive with electron cyclotron waves. Giruzzi[13] gave a simple analytical formula to express the current drive efficiency, and showed a significant degradation of the current generated away from plasma axis due to the trapping effect. Cohen,[14] in his work, gave the trapped-particle effects on electron cyclotron resonance heating and lower hybrid current drive using the adjoint formalism. His calculations illustrate the mutual effects of ECRH and LHCD on flux surfaces in tokamaks. In this paper, trapped electron effects on off-axis LHCD and rf power absorption by electrons

*Project supported by the National Natural Science Foundation of China (Grant Nos 10675043, 10575031 and 10675042).
†E-mail: jiaoym@swip.ac.cn

in the resonance regime at the tail of the distribution function are investigated. The analysis utilizes a 2D velocity space Fokker Planck code rather than an adjoint technique for studying the effects of particle trapping in LHCD. We emphasize the influences of the resonance regime and the trapped particle fraction on the current drive efficiency. This is relevant to velocity space distribution at a given magnetic surface.

2. Trapping effect in tokamak devices

In a tokamak configuration, particles can be divided into passing particles and trapped particles (see Ref.[15]). The trapped particles are trapped on the low magnetic field side of a tokamak, where the region can be considered as a magnetic mirror. The magnitude field in a tokamak is

$$B_\varphi = B_0(1-\varepsilon\cos\theta), \tag{1}$$

where $\varepsilon = r/R_0$, and the particles satisfying

$$\frac{v_{//}^2}{v_\perp^2} < \frac{2\varepsilon}{1-\varepsilon} \tag{2}$$

are trapped. The fraction of trapped particles is

$$f_{\rm T} = \sqrt{\frac{2\varepsilon}{1+\varepsilon}} \tag{3}$$

for a Maxwellian distribution.

Using equation $J = \oint mv_{//}\mathrm{d}l$, we can obtain toroidal drift velocity of a trapped electron[16]

$$v_\varphi = \frac{\Delta R_0\varphi}{\tau_b} = \frac{mv_\perp^2 q}{eB_\varphi r}\Big[\Big(\frac{E(k)}{K(k)} - \frac{1}{2}\Big) + \frac{2q'r}{q}\Big(\frac{E(k)}{K(k)} - 1 + k^2\Big)\Big], \tag{4}$$

where, $q = rB_\varphi/(RB_\theta)$ is the safety factor; $K(k)$ and $E(k)$ are

$$K(k) = \int_0^{\pi/2} \frac{\mathrm{d}x}{(1-k^2\sin^2 x)^{1/2}},$$
$$E(k) = \int_0^{\pi/2} (1-k^2\sin^2 x)^{1/2}\mathrm{d}x,$$
$$k^2 = \frac{W-\mu B_0(1-\varepsilon)}{2\varepsilon\mu B_0}. \tag{5}$$

$k^2 \approx (1/(2\varepsilon))(v_{//}^2/v_\perp^2) < 1$ is for the trapped electrons. And the reversal angle $\theta_{\rm M}$ satisfies $\cos\theta_{\rm M} = 1-k^2$. v_φ decreases as $\theta_{\rm M}$ decreases, thus as k^2 decreases, and when $k^2 \to 0$, v_φ runs to the value $mv^2q/(2eB_\varphi r)$. The toroidal drift speed of a trapped electron is always less than its thermal speed, and the bouncing motion has a block effect on current drive.

Now we consider the number of trapped electrons in the resonance regime $[v_{//1}, v_{//2}]$, which satisfies inequality (2)

$$n_{\rm trap} = 2\pi\int_{v_{//1}}^{v_{//2}}\int_{\sqrt{\frac{1-\varepsilon}{2\varepsilon}}v_{//}}^{\infty} v_\perp f(v_{//}, v_\perp)\mathrm{d}v_\perp\mathrm{d}v_{//}. \tag{6}$$

The total number of electrons in the resonance regime $[v_{//1}, v_{//2}]$ is

$$n_{\rm res} = 2\pi\int_{v_{//1}}^{v_{//2}}\int_0^{\infty} v_\perp f(v_{//}, v_\perp)\mathrm{d}v_\perp\mathrm{d}v_{//}. \tag{7}$$

Here, $2\pi\int_{-\infty}^{\infty}\int_0^{\infty} v_\perp f(v_{//},\, v_\perp)\mathrm{d}v_\perp\mathrm{d}v_{//} = 1$, and the speeds are normalized with the thermal speed $v_{\rm Te} = \sqrt{2T_{\rm e}/m_{\rm e}}$.

Table 1. The trapped particle fraction in the resonance regime.

$[v_{//1}, v_{//2}]$	D_0	$\varepsilon = r/R_0$	$n_{\rm trap}$	$n_{\rm res}$	$n_{\rm trap}/n_{\rm res}$
[0.0, 15]	0.0	0.2	0.2551	0.4962	0.5141
[1.0, 15]	0.0	0.2	0.0276	0.1558	0.1771
[1.0, 15]	1.0	0.2	0.0252	0.5716	0.0441
[2.0, 15]	0.0	0.2	2.58×10^{-4}	0.0226	0.0114
[2.0, 15]	1.0	0.2	7.21×10^{-4}	0.1210	0.0060
[2.5, 15]	0.0	0.2	7.94×10^{-6}	0.0062	0.0013
[2.5, 15]	1.0	0.2	3.11×10^{-5}	0.0281	0.0011
[3.0, 15]	0.0	0.2	1.10×10^{-7}	1.38×10^{-3}	8.03×10^{-5}
[3.0, 15]	1.0	0.2	1.71×10^{-7}	6.19×10^{-3}	2.76×10^{-5}
[1.0, 15]	0.0	0.4	0.0688	0.1560	0.4410
[1.0, 15]	1.0	0.4	0.1130	0.4250	0.2660
[2.0, 15]	0.0	0.4	0.0036	0.0226	0.1570
[2.0, 15]	1.0	0.4	0.0066	0.0767	0.0860
[3.0, 15]	0.0	0.4	3.66×10^{-5}	0.0014	0.0266
[3.0, 15]	1.0	0.4	1.09×10^{-4}	0.0055	0.0197

where $T_{\rm e} = 1$ keV.

Table 1 gives the fraction of the trapped electrons in the resonance regime $[v_{//1}, v_{//2}]$. In the table, the first column gives the trapped electron fraction with the Maxwellian distribution, which fits Eq.(2). We can also see that the fraction of the trapped electrons increases rapidly as the lower limit of the resonance regime (LLRR) is downshifted, and that the resonance electron fraction and trapped electron fraction become very small when the LLRR is larger than 3.0. With LHCD, the trapped electron ratio decreases, but the trapped electron number slightly increases. This indicates that part of the LH power is deposited on the low energy trapped electrons and thus they turn into passing electrons. The lower hybrid waves drive current by moving electrons out of the trapping regime instead of into it.

3. Fokker–Planck analysis

The general Fokker–Planck equation about the wave heating and current drive can be given as[6,7,9−11]

$$\frac{\partial f}{\partial t} = \Big(\frac{\partial f}{\partial t}\Big)_{\rm c} + Q + S, \tag{8}$$

where the first term on the right-hand side is the Fokker–Planck operator, and the particle source S is defined in Ref.[17]. The quasilinear operator can be expressed with the speeds $v_{//}$ and $v_\perp$ as

$$Q = \frac{1}{v_\perp}\frac{\partial}{\partial v_\perp}\Big[v_\perp\Big(D_{22}\frac{\partial f}{\partial v_\perp} + D_{21}\frac{\partial f}{\partial v_{//}}\Big)\Big] + \frac{\partial}{\partial v_{//}}\Big[D_{12}\frac{\partial f}{\partial v_\perp} + D_{11}\frac{\partial f}{\partial v_{//}}\Big]. \tag{9}$$

where $D_{12} = D_{21}$. Because LHH and LHCD are only induced through $v_{//} = \omega/k_{//}$ resonance energy transform, the quasilinear diffusion tensor only has the term of $v_{//}v_{//}$. Introducing $D \equiv D_{11}$, we obtain

$$\Big(\frac{\partial f}{\partial t}\Big)_{\rm LH} = \frac{\partial}{\partial v_{//}} D \frac{\partial}{\partial v_{//}} f, \tag{10}$$

where

$$D = \pi\frac{e^2}{m_{\rm e}^2}\int {\rm d}k_{//}|\tilde{E}_k|^2\frac{k_{//}^2}{k_\perp^2}\delta(\omega - k_{//}v_{//})$$

for $c/n_{//\rm M} < v_{//} < c/n_{//\rm m}$, and $D = 0$ otherwise.

The resonance condition is

$$\omega - v_{//}k_{//} = 0. \tag{11}$$

By using the code FPPAC developed from the two-dimensional Fokker–Planck package edited by McCoy *et al*,[17] to numerically solve Eq.(8), we can obtain the electron speed distribution function, and then the driven current density and power deposition density

$$J_{\rm rf} = -en_{\rm e}v_{\rm Te}\int_{v_{//1}}^{v_{//2}} v_{//}f(v_{//}){\rm d}v_{//},$$

$$P_{\rm abs} = \frac{1}{2}n_{\rm e}m_{\rm e}\nu_0 v_{\rm Te}^2\int_{v_{//1}}^{v_{//2}} v_{//}^2\frac{\partial}{\partial v_{//}}D\frac{\partial f}{\partial v_{//}}{\rm d}v_{//}, \tag{12}$$

where $v \to v/v_{\rm Te}$, and $t \to t\nu_0$. As a simple model, we can take the quasilinear coefficient as a constant (D_0). The Brambilla spectrum and the toroidal effect determine the injecting wave resonance regime and its power distribution.

For the LHCD case, the wave mainly accelerates the electrons along magnetic field lines. We obtain an obvious anisotropic energy deposition in accordance with the electron distribution function (see Fig.1).

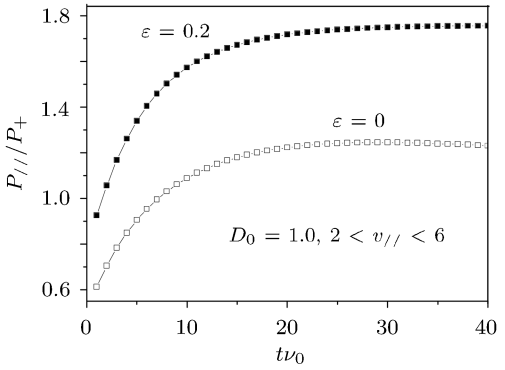


Fig.1. Anisotropic energy depositions under different trapping effects.

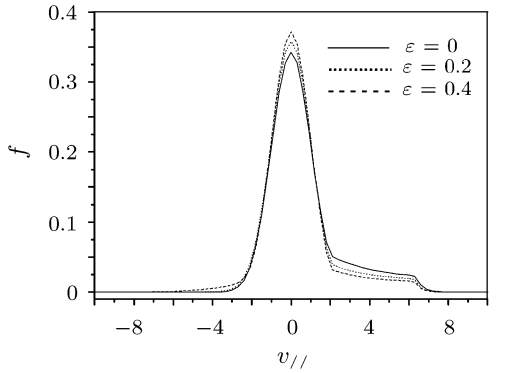


Fig.2. Electron velocity distribution functions with different trapping effects.

Figure 2 shows the electron velocity distribution functions with different trapping effects under LHCD. The electron distribution function deviates from the Maxwellian distribution clearly. From Fig.2 we can see that the trapped electrons consume more rf power,

which makes a lower flat resonance regime which represents the driven current.

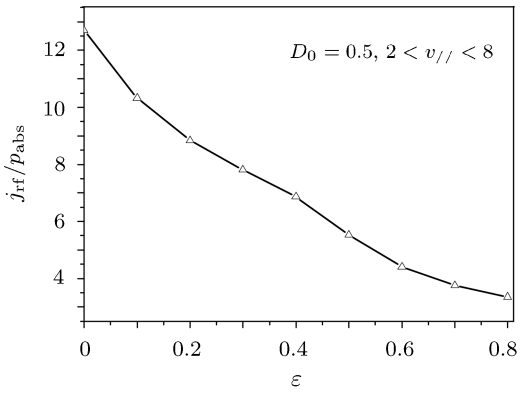


Fig.3. Current drive efficiencies with different trapping effects.

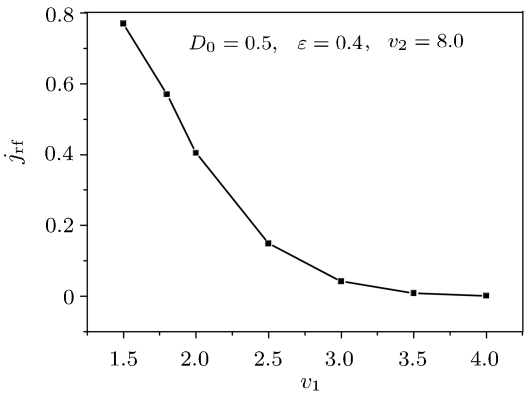


Fig.4. Driven currents with different LLRRs.

The results from a numerical simulation are given in Table 2, from which, we can see the relationship between trapping effect and plasma parameter. LHCD efficiency decreases as the trapping effect increases (see Fig.3), which is determined largely by the lower velocity limit of the resonance regime. The broadening of resonance regime, of course, benefits the current drive. Figure 4 shows the driven currents with different lower limits of resonance regime. The current decreases as the resonance regime lower limit increases. Figure 5 gives the current drive efficiencies with different lower limits of resonance regime When the LLRR is below 2.5, the trapping effect has a dominant effect, but the driving efficiency and driven current are high for very low LLRRs, because of the large numbers of resonance electrons. When LLRR is 2.0–2.5 the current drive efficiency is low. When it is higher than 2.5, the trapping effect gradually reduces, and the drive efficiency is high for very high LLRRs, but the driven current is low because of the small resonance regime and low 'plateau' in the velocity space. Because of the lower parallel velocity of trapped electrons, trapped electron fraction decreases with the raising of the LLRR, but current drive needs a relatively low value of the lower limit parallel velocity, so that we must distinguish the effects of resonance electron number from the trapping effect. Generally, trapping effect can cut the current drive efficiency by 30% (see Table 2).

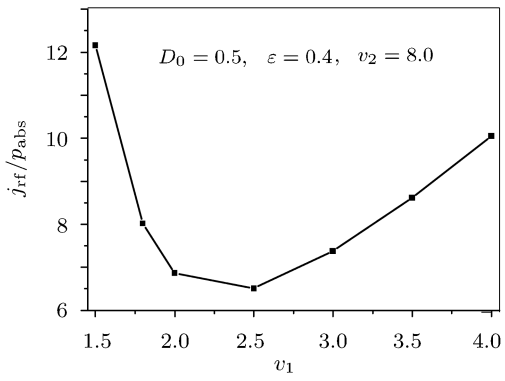


Fig.5. Current drive efficiencies with different LLRRs.

Table 2. Numerical simulation results for LHCD.

D_0	$[v_{//1}, v_{//2}]$	$\varepsilon = r/R_0$	$j_{\rm rf}$	$p_{\rm abs}$	$j_{\rm rf}/p_{\rm abs}$
0.5	[2.0,6.0]	0.0	0.8779	0.0740	11.85
0.5	[2.0,6.0]	0.2	0.3619	0.0547	6.709
0.5	[2.0,8.0]	0.0	1.2140	0.0946	12.38
0.5	[2.0,8.0]	0.2	0.5747	0.0639	8.994
0.5	[3.5,8.0]	0.0	0.0267	0.0018	15.13
0.5	[3.5,8.0]	0.2	0.0159	0.0013	12.16
0.5	[2.0,8.0]	0.0	1.2140	0.0946	12.83
0.5	[2.0,8.0]	0.4	0.4216	0.0581	7.252
1.0	[2.0,8.0]	0.0	1.9220	0.1298	14.80
1.0	[2.0,8.0]	0.4	0.5737	0.0544	10.54

Where $T_{\rm e} = 1$ keV and $j_{\rm rf} = \int_{v_{//1}}^{v_{//2}} v_{//} f(v_{//}) {\rm d}v_{//}$, $p_{\rm abs} = \nu_0 D_0 \int_{v_{//1}}^{v_{//2}} v_{//}^2 \dfrac{\partial^2 f}{\partial v_{//}^2} {\rm d}v_{//}$.

4. ITER scaling law estimation

Lower hybrid waves undergo strong single-pass damping in an ITER-like tokamak with the damping location being determined by the condition $v_{//}/v_{\rm Te} \sim 2.5$.[6,7,9,10] This condition can be used to determine the peak value for the $n_{//}$ spectrum. The lower limit phase speed of the power spectrum can be set below this condition, but must avoid absorbing by electron landau damping (ELD). The upper limit phase speed can be set by the condition of lower hybrid (LH) wave accessibility. The two conditions can be used to restrict the LH deposition location to $r/a = 0.6 - 0.8$ in off-axis current profile control for the typical parameters. The trapping effect must be considered in this region.

We assume the density and temperature profiles to be as follows:

$$n_{\rm e}(r) = n_{\rm e0}(1-(r/a)^2)^{\alpha_{\rm n}},$$
$$T_{\rm e}(r) = T_{\rm e0}(1-(r/a)^2)^{\alpha_{\rm T}}, \qquad (13)$$

where $n_{\rm e0}$ and $T_{\rm e0}$ are the density and temperature at plasma centre. The choice of the coefficients $\alpha_{\rm n}$ and $\alpha_{\rm T}$ depends on the distinct discharge conditions, which can be chosen as peaking or flattening profiles.

According to quasilinear theory and ignoring the DC electric field, ITER experiential scale gives the current drive efficiency[18]

$$\eta_{\rm cd} \equiv \bar{n}_{\rm e} R_0 I_{\rm p}/P_{\rm d} = \gamma_0 F(x, Z_{\rm eff}) G(\varepsilon, x), \qquad (14)$$

where γ_0 is the Fisch–Boozer factor

$$\gamma_0 = \frac{2m_{\rm e}\varepsilon_0^2 c^2}{e^3 \ln\Lambda} \frac{1}{\langle n_{//}\rangle^2} \frac{4}{5+Z_{\rm eff}}$$
$$\frac{1}{\langle n_{//}\rangle^2} = \Big[\frac{1}{n_{//\,\min}^2} - \frac{1}{n_{//\,\max}^2}\Big] \Big/ \ln\Big[\frac{n_{//\,\max}^2}{n_{//\,\min}^2}\Big]; \qquad (15)$$

$F(x, Z_{\rm eff})$ is the temperature factor

$$F(x, Z_{\rm eff}) = 1 + \frac{1}{x^2}\Big[\frac{5+Z_{\rm eff}}{4} + \frac{3}{2}\frac{6+Z_{\rm eff}}{3+Z_{\rm eff}}\Big] + \frac{1}{x^3}\frac{3\sqrt{2\pi}(5+Z_{\rm eff})}{8Z_{\rm eff}}; \qquad (16)$$

$G(\varepsilon, x)$ is trapping effect

$$G(\varepsilon, x) = 1 - \frac{\varepsilon^{0.77}(12.25+x^2)^{0.5}}{3.5\varepsilon^{0.77}+x}, \qquad (17)$$

where $x = c/(\langle n_{//}\rangle v_{\rm th})$ and $v_{\rm th} = \sqrt{T_{\rm e}/m_{\rm e}}$.

From Figs.6 and 7, it is clear that the accessibility condition is mainly determined by plasma density and easily satisfied in the off-axis current drive, since the required $n_{//}$ value decreases with the minor radius increasing. The major issue in off-axis current drive is the power deposition since we want it to be located at about $r/a = 0.6 - 0.8$. From quasilinear theory, the power spectrum peak value must be located near $v_{//}/v_{\rm Te} \sim 2.5$. This corresponds to $\varepsilon = 0.15 - 0.2$, $\langle n_{//}\rangle = 8.15 - 14.48$ for HL-2A, and $\varepsilon = 0.19 - 0.26$, $\langle n_{//}\rangle = 3.16 - 5.62$ for ITER respectively. Using the ITER scaling law, expression (17), we obtain $G = 0.77 - 0.72$ for HL-2A, and $G = 0.68 - 0.66$ for ITER, the trapping effect cuts the current drive efficiency by about 30%.

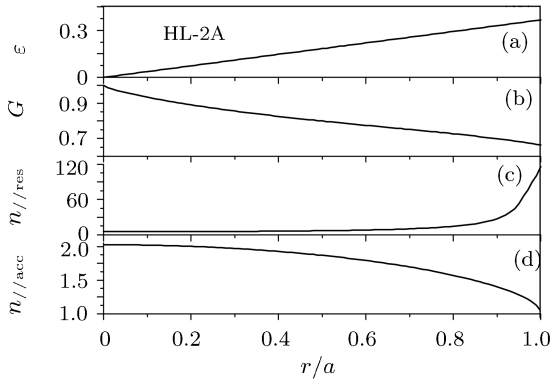


Fig.6. Parameter profiles for HL-2A with $\alpha_{\rm n} = 1$, $\alpha_{\rm T} = 2$ and $n_{\rm e0} = 5 \times 10^{19}$ m^{-3}, $T_{\rm e0} = 1.5$ keV: (a) reverse aspect ratio, (b) trapping factor defined in expression (17), (c) $n_{//}$ index given by quasilinear absorption, (d) $n_{//}$ index given by accessibility.

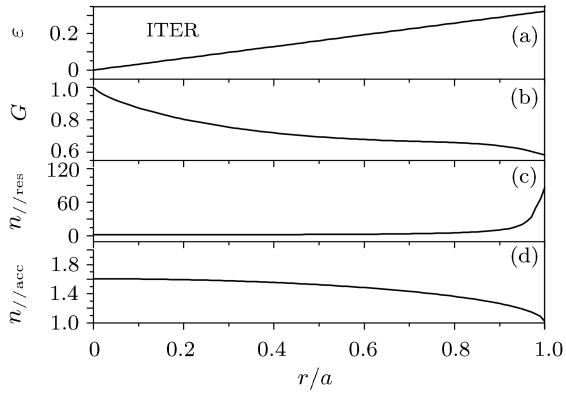


Fig.7. Parameter profiles for ITER with $\alpha_{\rm n} = 1$, $\alpha_{\rm T} = 2$ and $n_{\rm e0} = 1 \times 10^{20}$ m^{-3}, $T_{\rm e0} = 10$ keV: (a) reverse aspect ratio, (b) trapping factor defined in expression (17), (c) $n_{//}$ index given by quasilinear absorption, (d) $n_{//}$ index given by accessibility.

Because the $\varepsilon = r/R$ increases along the minor radius and equals zero at the plasma centre, the trapping effect happens only in the off-axis current drive. In an ITER-like large tokamak (with $R = 6.2$ m and

$a = 2.0$ m), because of its high density and high temperature, the off-axis current drive can be easily obtained by the 'grill' in the general power spectrum: for example, $n_{//} \subset [2.0, 8.0]$. But in HL-2A-like middle scale tokamak (with $R = 1.64$ m and $a = 0.4$ m), because of its low density and low temperature, the off-axis current drive needs higher $n_{//}$ spectrum, for example, $n_{//} > 8.0$. This is difficult to reach in the general 'grill' spectrum, but perhaps can be obtained by tokamak toroidal effect. In this case, $v_{//}/v_{\mathrm{Te}}$ is very low (see Table 1) and the trapping effect must be considered.

5. Discussion and conclusions

Wave accessibility in a plasma depends on plasma conditions and wave properties. The eikonal method[9,10] is used to study the lower hybrid wave propagation in tokamak plasmas. The ray equations describing the trajectory of a wave packet are obtained from the local dispersion relation $D(\boldsymbol{x}, \boldsymbol{k}, \omega) = 0$, where $\omega, \boldsymbol{k}$ and D are real in calculating the ray trajectory. In a tokamak configuration, the ray equations are written as

$$\begin{aligned}
&\frac{\mathrm{d}r}{\mathrm{d}t} = -\frac{\partial D/\partial k_r}{\partial D/\partial \omega}, \quad \frac{\mathrm{d}k_r}{\mathrm{d}t} = \frac{\partial D/\partial r}{\partial D/\partial \omega},\\
&\frac{\mathrm{d}\theta}{\mathrm{d}t} = -\frac{\partial D/\partial m}{\partial D/\partial \omega}, \quad \frac{\mathrm{d}m}{\mathrm{d}t} = \frac{\partial D/\partial \theta}{\partial D/\partial \omega},\\
&\frac{\mathrm{d}\varphi}{\mathrm{d}t} = -\frac{\partial D/\partial n}{\partial D/\partial \omega}, \quad \frac{\mathrm{d}n}{\mathrm{d}t} = \frac{\partial D/\partial \varphi}{\partial D/\partial \omega} = 0, \qquad (18)
\end{aligned}$$

where r is the radius measured from the magnetic axis of the torus, θ is the poloidal angle, and φ is the toroidal angle. Conjugate wave number variables are k_r, $m = rk_\theta$, and $n = (R_0 + r\cos\theta)k_\varphi$ with R_0 being the major radius. In terms of these variables, we have

$$\begin{aligned}
k_{//} &= \Big[k_r B_r + \Big(\frac{m}{r}\Big)B_\theta + \frac{nB_\varphi}{(R_0 + r\cos\theta)}\Big]|\boldsymbol{B}|^{-1},\\
k_\perp^2 &= k_r^2 + \Big(\frac{m}{r}\Big)^2 + \Big(\frac{n}{R_0 + r\cos\theta}\Big)^2 - k_{//}^2. \qquad (19)
\end{aligned}$$

The equations clearly show that for a tokamak equilibrium with poloidal inhomogeneity and axial symmetry, the poloidal mode number is not conserved, whereas the toroidal mode number is a constant of the wave motion, i.e. along the ray trajectory wave momentum changes. Therefore, there exist various resonance regimes at difference magnetic surfaces. We can hardly obtain an analytic expression for a resonance regime on a local magnetic surface because of its dependence on tokamak parameters. With the initial power spectrum given by the launcher, we can obtain the ray trajectory and its $k_{//}$ or $n_{//}$ value, and then the resonance speed $v_{//} = c/n_{//}$ by numerically solving Eq.(18).

The resonance regimes on local magnetic surfaces are required in the views of plasma current profile control by LHCD. These can be obtained from the combination of tokamak magnetic configuration and ray tracing technology.[1−5,19] Spectral broadening and trapped electron effect are the two aspects of the toroidal effects. Detailed ray trajectory analysis may provide beneficial application of off-axis lower hybrid current drive. Such work is in progress and will be presented separately in the near future.

References

[1] Ekedahl A, Baranov Yu F, Dobbing J A, Fischer B, Gormezano C, Jones T T C, Lennholm, M, Parail V V, Rimini F G,, Romero G A, Schild P, Sips A C C, Söldner F X and Tubbing B J D 1998 *Nucl. Fusion* **38** 1397

[2] Goniche M, Grosman A, Aniel T, Michelis C De, Gunn D, Mazon D, Schunke B, Sgui J L and Vallet J C 2004 *Plasma Phys. Control. Fusion* **46** 899

[3] Sakamoto M, Itoh S, Sato K N, Nakamura K, Zushi H, Hanada K, Jotaki E, Makino K, Kawasaki S and Nakashima H 2000 *Nucl. Fusion* **40** 453

[4] Peysson Y and Tore Supra Team 2001 *Nucl. Fusion* **41** 1703

[5] Tala T J J, Söldner F X, Parail V V, Baranov Yu F, Heikkinen J A and Karttunen S J 2000 *Nucl. Fusion* **40** 1635

[6] Fisch N J 1978 *Phys. Rev. Lett.* **41** 873

[7] Fisch N J 1987 *Rev. Mod. Phys.* **59** 175

[8] Brambilla M 1976 *Nucl. Fusion* **16** 47

[9] Bonoli P T and Englade R C 1986 *Phys. Fluids* **29** 2937

[10] Imbeaux F and Peysson Y 2005 *Plasma Phys. Control. Fusion* **47** 2041

[11] Bernabei S and Ignat D W 1982 *Nucl. Fusion* **22** 735

[12] Yoshioka K and Antonsen T M 1986 *Nucl. Fusion* **26** 839

[13] Giruzzi G 1987 *Nucl. Fusion* **27** 1933

[14] Cohen R H 1987 *Phys. Fluids* **30** 2442

[15] Wesson J A 1997 *Tokamak* 2nd edn (Oxford: Clarendon)

[16] Kadomstv B B and Pogutse O P 1970 *Review of Plasma Physics* ed M. A. Leontovich, translated by H Lashinsky (New York/London: Consultants Bureau) **5** 265

[17] McCoy M G 1981 *Comput. Phys. Commun.* **24** 37

[18] Post D E 1991 *IAEA/ITER/DS/21* (International Atomic Energy Agency, Vienna) p196

[19] Ding B J, Shan J F, liu F K, Fang Y D, Wei W, Wu Z W, Chen Z Y, Xu H D, Wang M, Jiang M, Zhang G R, Huang F, Zhao Y P, Kuang G L and the HT-7 team 2006 *Chin. Phys.* **15** 2989